Low-Cost Bio-Based Phase Change Materials as an Energy Storage Medium in Building Envelopes

Kaushik Biswas[1], Nitin Shukla[2], Jan Kosny[2], Ramin Abhari[3]

[1] Energy and Transportation Science Division, Oak Ridge National Laboratory, Oak Ridge, TN, USA
[2] Building Energy Technologies Group, Fraunhofer Center for Sustainable Energy Systems CSE, Boston, MA, USA
[3] Renewable Energy Group Synthetic Fuels, LLC (formerly Syntroleum), Tulsa, OK, USA

Abstract: A promising approach to increasing the energy efficiency of buildings is the implementation of phase change material (PCM) in building envelope systems. Several studies have reported the energy saving potential of PCM in building envelopes. However, wide application of PCMs in building applications has been inhibited, in part, by their high cost. This article describes a novel paraffin product made of naturally occurring fatty acids/glycerides trapped into high density polyethylene (HDPE) pellets and its performance in a building envelope application, with the ultimate goal of commercializing a low-cost PCM platform. The low-cost PCM pellets were mixed with cellulose insulation, installed in external walls and field-tested under natural weatherization conditions for a period of several months. In addition, several PCM samples and PCM-cellulose samples were prepared under controlled conditions for laboratory-scale testing. The laboratory tests were performed to determine the phase change properties of PCM-enhanced cellulose insulation both at microscopic and macroscopic levels.

This article presents the data and analysis from the exterior test wall and the laboratory-scale test data. PCM behavior is influenced by the weather and interior conditions, PCM phase change temperature and PCM distribution within the wall cavity, among other factors. Under optimal conditions, the field data showed up to 20% reduction in weekly heat transfer through an external wall due to the PCM compared to cellulose-only insulation.

Key words: phase change materials, low-cost PCM, PCM-cellulose insulation

1. INTRODUCTION

PCMs in building envelopes operate by changing phase from solid to liquid while absorbing heat from the outside and thus reducing the heat flow into the building, and releasing the absorbed heat when it gets cold outside reducing the heat loss through the building envelope. The energy saving potential of PCMs for buildings has been demonstrated [1, 2], but the traditionally high PCM prices have precluded extensive application of PCMs in the building industry.

This project was initiated in 2010 by Syntroleum Corporation, in response to a funding opportunity announcement by the U.S. Department of Energy. The major goal was to fundamentally change the manufacture of phase change material (PCM) and develop a low-cost PCM platform. The proposed low cost process involves a sustainable and more selective route to PCM paraffins and a low cost approach to converting the paraffins to form-stable PCM pellets. The low cost PCM production process involves two components: (1) on-purpose production of

C16-C18 paraffins from low cost bio-renewable feedstocks, and (2) low cost encapsulation using under-water pelletizers. Paraffins are straight chain saturated hydrocarbons with high latent heat. Hexadecane ($C_{16}H_{34}$), heptadecane ($C_{17}H_{36}$), and octadecane ($C_{18}H_{38}$) are three paraffins that melt/freeze between 18ºC (64ºF) and 28ºC (82ºF) [3, 4]. This temperature range is considered the comfort zone for most people. High latent heat and suitable phase change temperature range make these paraffins attractive as PCMs for building applications.

Animal fats and vegetable oils are 97% or higher C_{16} and C_{18} fatty acids, and can be converted to C_{16}-C_{18} paraffins using a reaction called hydrodeoxygenation. Further, studies have shown that paraffins can be trapped into high density polyethylene (HDPE) by co-crystallizing a paraffin/HDPE melt. Up to 70% paraffin can be trapped in the HDPE matrix such that molten paraffin does not seep out of the solid HDPE matrix. Under-water pelletizers have been successfully used to convert molten polymer systems to pellets of various sizes, including < 1 mm pellets. The combination of C_{16}-C_{18} paraffin production from low value fats and waste vegetable oils, combined with low cost encapsulation via under-water pelletizers, is expected to result in a step-change in PCM production costs. For a payback period of 10 years, assuming 30%-by-weight dispersed PCM in wall insulation, Kosny et al. [5] estimated cost targets of $3.30-8.80/kg ($1.50-4.00/lb) for PCMs with latent heats varying between 120 to 220 kJ/kg. The cost of the current PCM with a latent heat of 116 kJ/kg [6] is projected to be about $4.40-6.60/kg ($2-3/lb) or less, when manufactured at a commercial scale.

Syntroleum collaborated with Oak Ridge National Laboratory to field-test their PCMs in one of ORNL's test facilities located in Charleston, SC. A test was built and installed with different combinations of cellulose and PCM containing HDPE pellets as cavity insulation. The wall was instrumented with temperature, humidity and heat flux sensors for monitoring. In parallel, laboratory tests were performed by Fraunhofer Center for Sustainable Energy Systems (CSE) under controlled conditions to characterize the thermal storage properties of the low-cost PCM. This article describes the testing and analysis from both the field and laboratory tests.

2. TEST FACILITY AND TEST WALL DETAILS

Figure 1. Charleston, SC NET facility.

The field testing was performed in a natural exposure test (NET) facility in Charleston, SC. The NET facility is temperature and humidity controlled and instrumented to measure moisture

content in materials, vapor pressure, temperature, heat flux, humidity, etc. Figure 1 shows the southeast wall of the NET facility, with multiple side-by-side test walls that are exposed to natural weathering. The test wall being described in this article was also built on the southeast wall. Also shown is a weather station on the southwest gable end of the building. During the test period, the indoor temperature was maintained at about 20-22°C.

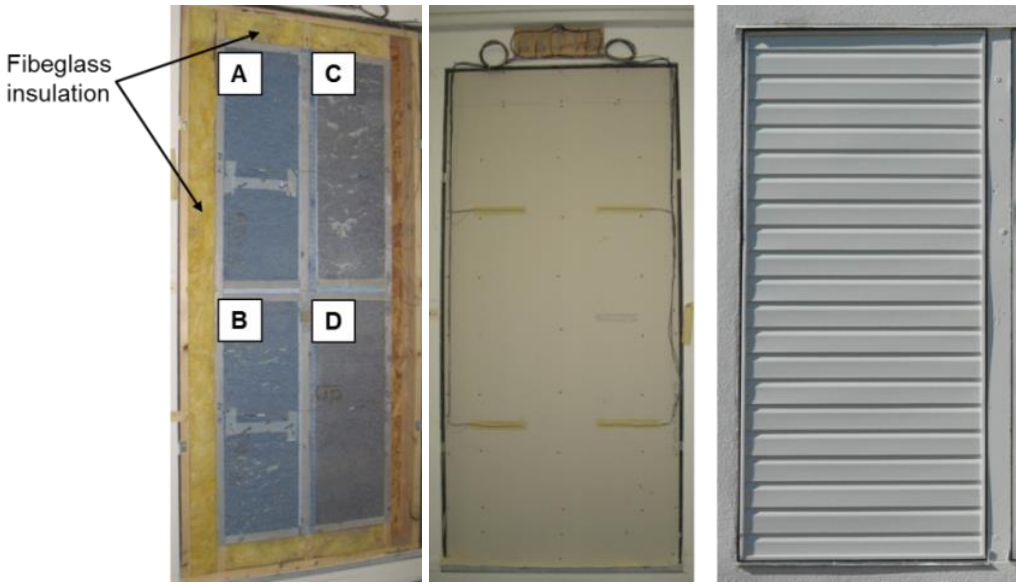

Figure 2. Left: Test wall – (A) cellulose-only insulation, (B) cellulose-HDPE mix, (C) cellulose-PCM mix, and (D) cellulose-PCM-cellulose sandwich structure; Center – Finished interior; Right – Finished exterior.

Figure 2 shows the test wall containing the PCM. The wall was built using 2 x 6 wood studs, resulting in a cavity depth of 14 cm (5.5 inch), with 1.2 cm (0.5 inch) oriented strand board (OSB) attached to the exterior side of the wall. The test wall was divided into four sections or wall cavities. The cavity dimensions were 1.1 x 0.4 m^2 (42.4 x 14.5 square inch). The nominal amount of PCM in the cellulose-PCM cavity (section C) was 20% by weight. The PCM-HDPE pellet design was such that the pellets contained 66% paraffin by weight. Thus, the PCM pellets and cellulose were mixed so that the mixture contained 31% of pellets, or 0.45 kg of pellets for each kg of cellulose. For the cavity with cellulose mixed with the HDPE pellets without PCM, the same volume ratio as the cellulose-PCM pellet mixture was maintained. In section D, a cellulose-PCM-cellulose sandwich configuration was used, as shown in Figure 3.

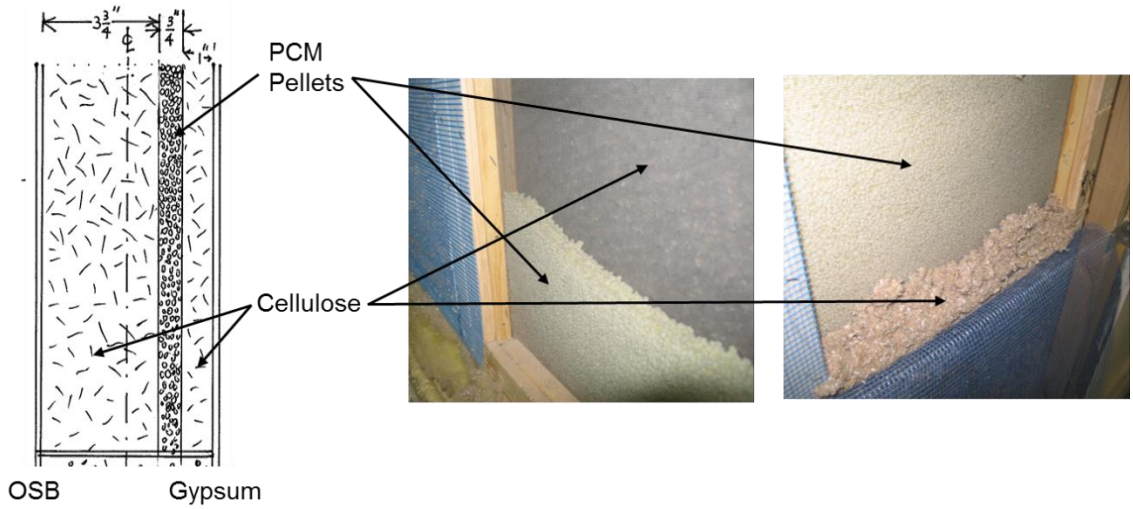

Figure 3. Cellulose-PCM sandwich structure.

Once installed, the outer cavities of the test wall were filled with fiberglass insulation to thermally insulate the wall from the other neighboring test walls, as shown in Figure 2. The interior side was covered with 1.3 cm (0.5 in) gypsum board and the exterior OSB was covered with a weather resistive barrier (0.15 mm thick high density polyethylene sheet) underneath vinyl siding. Also visible on the interior face are four (4) temperature sensors, one centered on each cavity, which are further described in the next section.

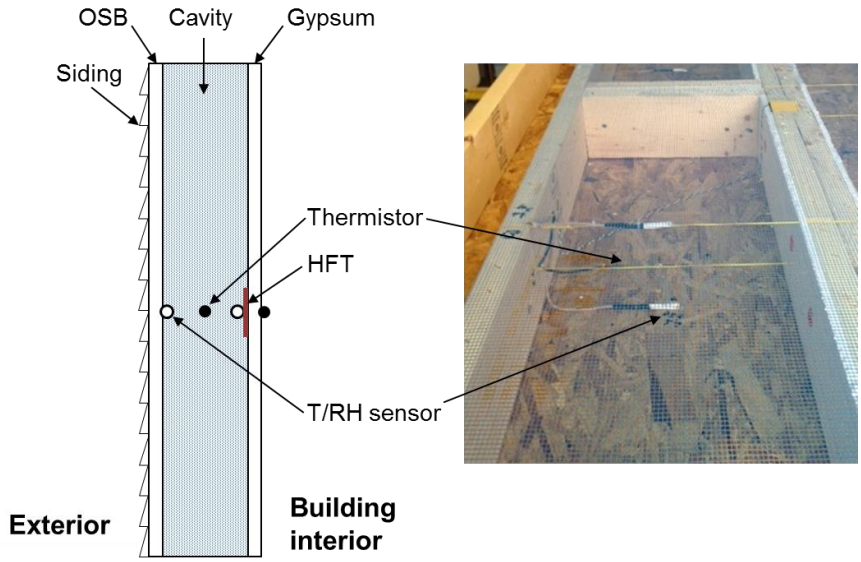

Figure 4. Sensor placement in test wall.

Figure 4 shows the typical instrumentation layout in the wall cavities. The wall contained vinyl siding and a weather barrier over OSB on the exterior side, and the interior side was covered with a gypsum board. Each cavity contained a thermistor and RH sensor combination (T/RH sensor) on the OSB and gypsum surfaces facing the cavity, thermistor inside the cavity (mid-depth) and on the gypsum surface facing the room interior, and a heat flux transducers (HFT) on

the gypsum surface facing the cavity. The HFTs were 2 x 2 inch. Within each cavity, these sensors were located approximately in a line along both the vertical and horizontal midpoints of the cavity. Also, a single thermistor was attached to the wall exterior (interior face of the siding) and a T/RH sensor combination on the OSB surface facing the exterior, which are not shown in Figure 4. The T/RH sensor is indicated by the white packets seen in Figure 4. In addition to the sensors attached to the test wall, the NET facility includes sensors and instruments to monitor the local weather conditions, including temperature, humidity and solar irradiance.

Each sensor was scanned at five minute intervals and the data were averaged and stored at hourly intervals. The data were downloaded on a weekly basis using a dedicated computer and modem. Table 1 provides the sensor specifications.

Table 1. Installed sensor accuracy.

Sensor	Accuracy	Sensitivity	Repeatability
10K ohm thermistor	± 0.2%	-	± 0.2%
Humidity sensor	± 3.5%	-	± 0.5%
Heat flux transducer	± 5%	(5.7 W/m^2)/mV	-
Solar pyranometer, vertical	± 3%	$0.2 \cdot kW \cdot m^{-2} \cdot mV^{-1}$	-

3. LABORATORY-SCALE PCM CHARACTERIZATION TESTS

(1) **Differential Scanning Calorimeter (DSC):** DSC tests were performed using two different modes: ramp and step methods. In ramp method, sample is subjected to a constant heating or cooling rate, and heat flow through the sample is measured. It is important to note that due to finite thermal mass of the sample, thermal response of the DSC may lag behind the ramp input, resulting in a ramp rate dependent heat capacity data [5]. In step method, sample temperature is changed in increments or steps, and heat flow during the step change is measured. Step method gives very accurate measurement of PCM enthalpy as a function of temperature, provided that sufficient time is given during each temperature step change ensuring negligible heat flow at the end of the of each measurement.

(2) **Dynamic Heat Flow Meter Apparatus (DHFMA):** DHFMA follows the same principle as the DSC step method but is applicable to large-scale samples such as building components. DHFMA test method utilizes temperature and heat flux information from a conventional HFMA to determine the dynamic thermal properties of PCM-enhanced components.

4. RESULTS AND DISCUSSION

Field Data Analysis: Figure 5 shows the measured temperatures within the different wall sections and heat flows through the different wall sections during a summer week. The sensor descriptions are based on their locations within the test wall. 'Interior' refers to any surface faced towards the building interior and 'Exterior' indicates any surface facing outside to the building exterior. In Figure 5, the 'Wall Exterior' is the thermistor located under the outer vinyl siding, 'OSB Interior' is the thermistor (T/RH combination) on the OSB surface facing the cavity, and 'Cavity' is the thermistor installed in the cavity center along its depth.

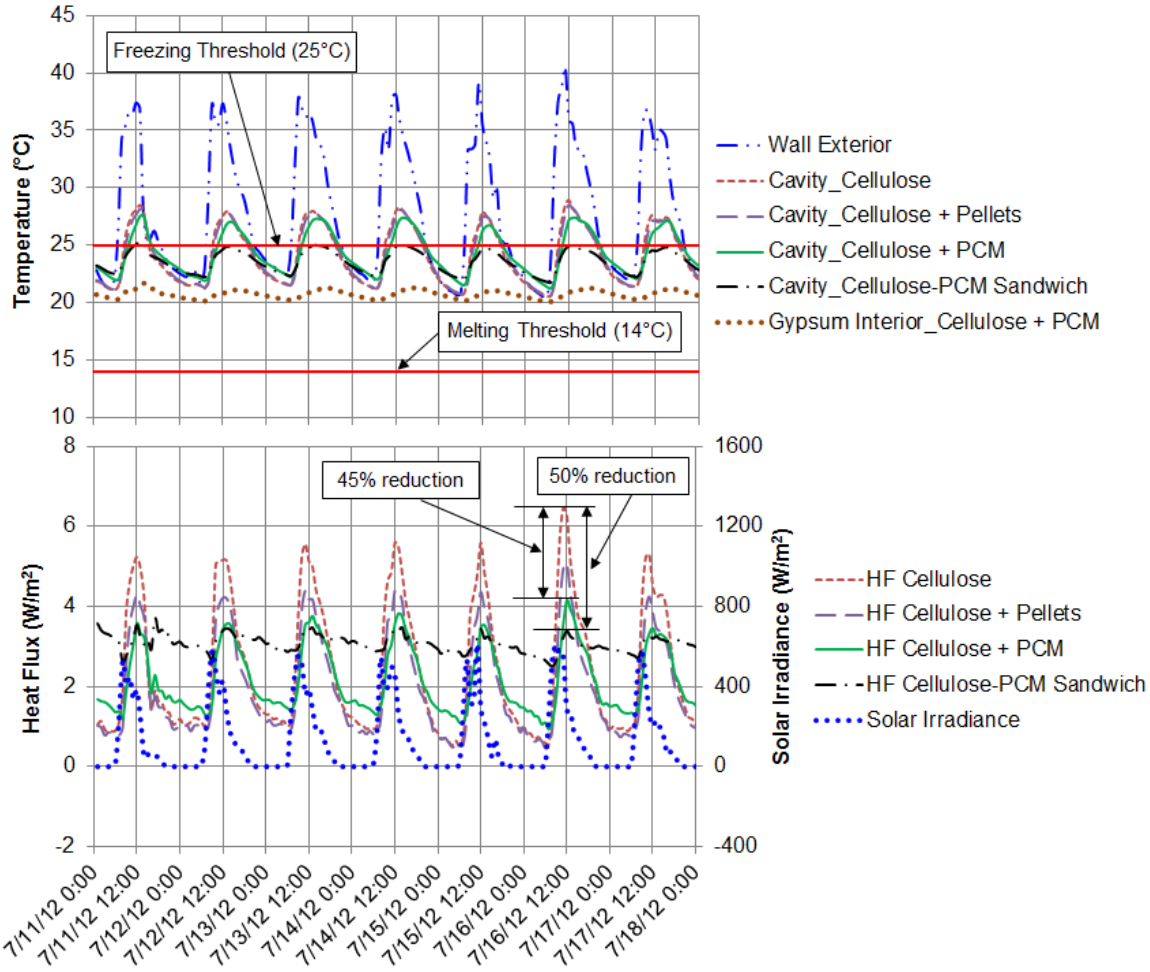

Figure 5. Temperature and heat flux variation for a week during summer.

To examine whether any phase change was occurring in the PCM sections, the threshold temperatures for initiation of melting and freezing have also been included. Melting threshold is the temperature at which the fully frozen PCM will start melting, and at freezing threshold a fully molten PCM will start freezing. The PCM phase change data shown in Figure 5 originally provided by the manufacturer based on some differential scanning calorimetry (DSC) testing in which the PCM sample were heated or cooled at 1°C per minute.

Figure 5 also shows the heat flux variations through the different sections and the south wall solar irradiance (right axis). The heat flux transducers (HFTs) were attached to the exterior surface of the gypsum board (facing the cavity). The sign convention of heat flux is such that heat flow through the gypsum board into the building interior (heat gain) is positive, while heat flow out of the building into the wall cavities (heat loss) is negative.

A substantial reduction in the peak heat gains, up to 45 and 50% in the cellulose-PCM and cellulose-PCM sandwich sections, respectively, was observed compared to the cellulose-only section. The heat flows were always into the building, but cellulose and cellulose-pellet sections had lower heat gains during the nights. This indicates some cooling energy penalty for the PCM containing sections at night, especially the cellulose-PCM sandwich section.

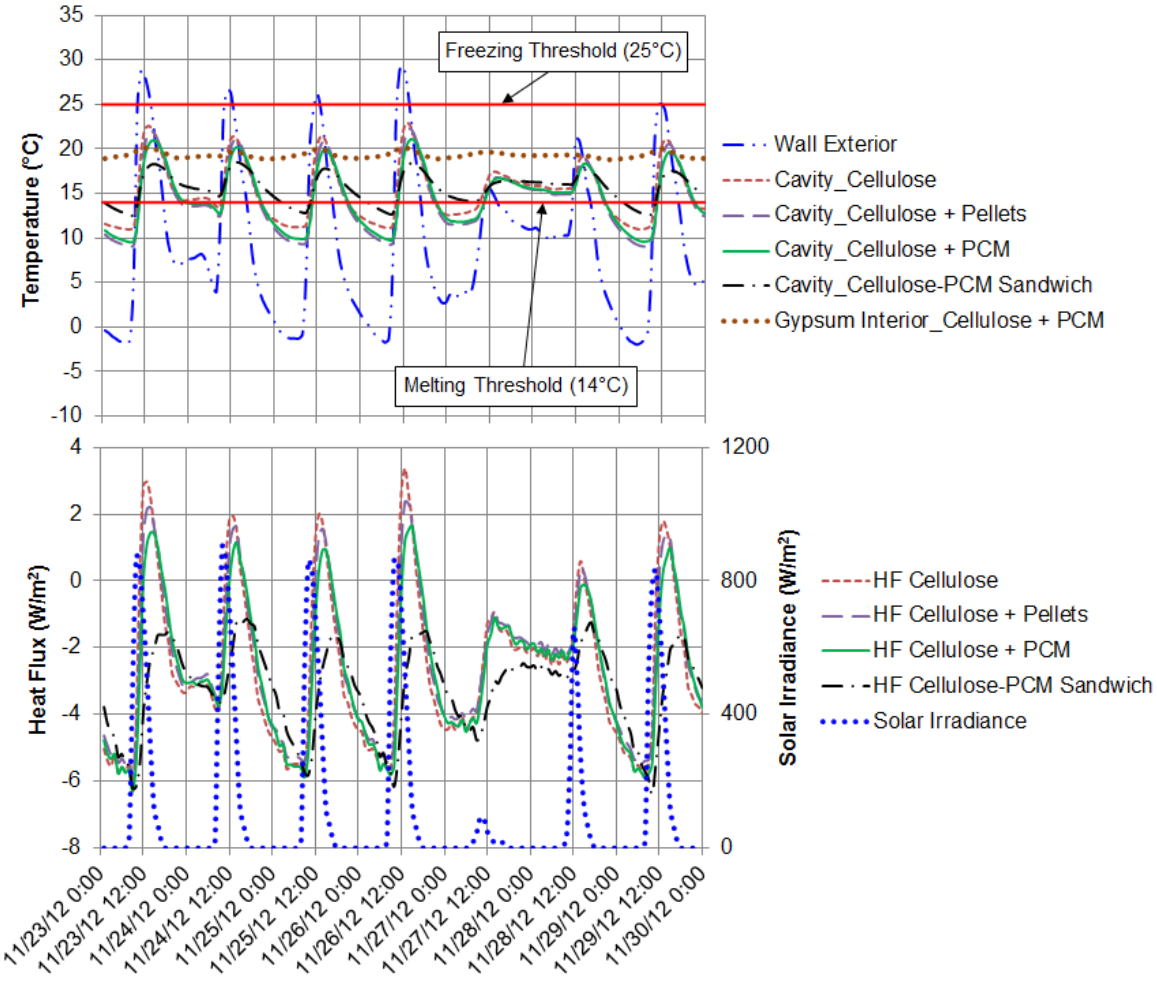

Figure 6. Temperature and heat flux variation for a week during the phase 2 winter period.

Figure 6 shows the temperatures and heat fluxes during a winter week. During this week, the heat flows were primarily out of the building. There was some daytime heat gain through all sections, except the cellulose-PCM sandwich section. The nighttime losses were similar through all sections. The lower daytime heat gains through the cellulose-PCM section and no heat gains at all through the cellulose-PCM-cellulose sandwich section indicate heating penalties compared to cellulose-only insulation.

To further investigate the impact of the PCM wall sections, the heat flux data were integrated over 30-day winter and summer periods to determine the total heat gains and losses through the different sections. The integration was performed by a simple application of the trapezoidal rule:

$$Total\ Integrated\ Heat\ Flow\ [\frac{kJ}{m^2}] = \sum_{n=0}^{m} 0.5 \cdot \Delta X_n \cdot (Y_n + Y_{n+1}) \qquad (1)$$

Where Y_n and Y_{n+1} correspond to the current and future time step, and ΔX_n is the time step (one hour in this case). The positive and negative heat fluxes were integrated separately to determine

the heat gains and losses for each section. The monthly integrated or total heat gains and losses and the net heat transfer are shown in Table 2. The net heat transfer for each period was obtained by integrating the positive and negative heat fluxes together. Also shown are the percent reductions with respect to the section with only cellulose insulation. The summer and winter periods considered are also listed in the tables.

Table 2. Integrated heat flow into and out of the conditioned space through the different sections.

Cavity	Heat Gain (kJ/m^2)	% Reduction	Heat Loss (kJ/m^2)	% Reduction	Net (kJ/m^2)	% Reduction
Summer 30-day period (Phase 2) (Jun 29 - Jul 28, 2012)						
Cellulose	7068.52		0.00		7068.52	
Cellulose + Pellets	5744.47	18.73	0.00		5744.47	18.73
Cellulose + PCM	6218.95	12.02	0.00		6218.95	12.02
Cellulose-PCM Sandwich	8438.94	-19.39	0.00		8438.94	-19.39
Winter 30-day period (Phase 2) (Nov 1 - 30, 2012)						
Cellulose	708.58		-5997.34		-5288.76	
Cellulose + Pellets	535.09	24.48	-5539.69	7.63	-5004.59	5.37
Cellulose + PCM	361.96	48.92	-5740.36	4.28	-5378.40	-1.69
Cellulose-PCM Sandwich	23.22	96.72	-6613.95	-10.28	-6590.73	-24.62

During the summer period, the cellulose-PCM section reduced the heat gains compared to the cellulose-only section by 12%. While the cellulose-PCM sandwich section was very effective in reducing the peak heat gains (Figure 5), it allowed higher total heat gain compared to the cellulose-only section. During the winter period, the cellulose-PCM section reduced the total heat loss by 4.28%, but also reduced the heat gains by almost 50% compared to the cellulose-only section. The heating penalty due to reduced daytime gains is reflected by a small increase (1.69%) in the net heat loss through the cellulose-PCM compared to the cellulose-only section. The cellulose-PCM sandwich section performed poorly during the winter period, with almost 25% higher total heat loss compared to the cellulose-only section. With the added thermal mass, the cellulose-pellets section actually performed better than all other wall sections by reducing both heat gains and losses during the summer and winter periods.

It should be noted that the heat fluxes were local, center-of-cavity values and did not necessarily reflect the energy-savings impact, or lack thereof, of the PCM-enhanced cellulose insulation. Also, the settling of insulation and the stratification of the PCM-containing HDPE pellets added further uncertainty to the local heat flux data (as explained below). There is a potential for uneven settling and density differences in the wall sections, which could impact the heat flows through the center of each section. The local heat flux data are not sufficient to accurately determine the energy-saving impact of the tested PCMs. Detailed energy modeling is required that captures all the building envelope features and indoor and ambient conditions to calculate the annual energy usage to estimate the energy benefits of the cellulose-PCM insulation.

Finally, one source of uncertainties in the measurements needs to be acknowledged. The cellulose-PCM and cellulose-pellets mixing and loading method was such that it was difficult to obtain a uniform distribution of the PCM pellets within the cellulose insulation. Figure 7 shows how the PCM pellets were concentrated in certain regions within the cavities.

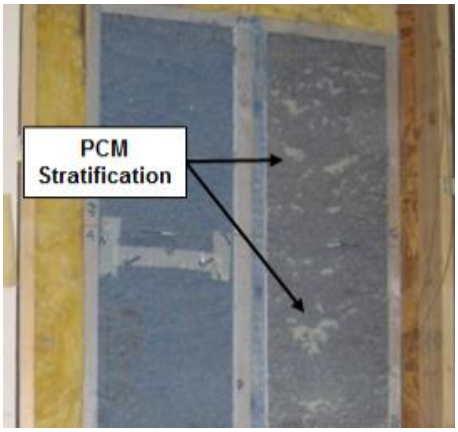

Figure 7. PCM stratification in the cellulose-PCM mixture.

How the PCM pellets were distributed with respected to the sensors can have an impact on the sensor readings. Mid-cavity temperatures were measured for a brief period by three thermistors located mid-depth in the cellulose-PCM cavity at three different vertical locations. The measured temperatures varied by about 5°C (9ºF) depending on the vertical location and PCM concentration. Such variability in distribution could also impact the measured heat flows through the PCM-containing sections.

PCM Thermal Storage Characterization: Small samples of PCM weighing 20-30 mg were prepared for DSC measurement. Figure 8 shows DSC results on PCM sample during melting phase-change. Ramp rates of 0.2, 1, 5 and 10ºC/min were used. It is observed that the enthalpy curve shifts to left and approaches closer to the step method results as the ramp rate is slowed. Results for ramp of 0.2ºC/min is found to be close to the step mode results with peaks of the two curves offset by ~0.5ºC, which is within the resolution of 0.5ºC used for the step mode. The enthalpy change during phase change is determined to be ~120 J/g.[1] Figure 9 shows DSC results during solidification process. Here we notice enthalpy profiles are quite different for ramps of 0.2, 1, 5 and 10ºC/min. The slowest ramp of 0.2ºC/min exhibits multiple peaks in the enthalpy curve with the first and the highest peaks occurring at ~24.5ºC and 23ºC, respectively. On the other hand, step mode gives three peaks in the enthalpy profile with both the first and the highest peak occurring at ~25ºC. The enthalpy change during solidification is measured to be ~95 J/g.

A HFMA instrument was next used to measure the heat capacity of large size samples of 20 cm x 20 cm in areal dimension. The thickness of sample was 4 mm. DSC data shows that temperature resolutions of less than 1ºC is required to capture the details of the specific heat curve in phase active region. However, existing HFMA instruments have poor accuracy for temperature steps smaller than 1ºC. To achieve temperature resolution of less than 1ºC without compromising the accuracy of experiments, two separate tests covering phase change region were performed for both melting and solidification processes. Each of these tests used the same temperature steps of 1.5ºC, while a difference of 0.75ºC was kept between the first set-points of the two tests. By

[1] Defining phase change regime for a real PCM appears to be arbitrary in scientific literature. In the solid phase, the heat capacity increases more or less linearly with the temperature unlike the liquid phase where it remains constant. This troduces uncertainty regarding selection of onset of melting or end of solidification process. Here we assumed that melting starts once deviation in heat capacity linear trend is more than 10%.

combining the test data from these separate tests, it was possible to obtain a temperature resolution of 0.75ºC. DHFMA data for large size sample is slightly off than the step data. The difference could be attributed to following reasons:

1) DSC and DHFMA resolutions are different (0.5 and 0.75ºC, respectively).
2) Microscopic and large size samples may have slightly different chemical composition.

Phase change component of the PCM investigated in this study is mainly octadecane. For the purpose of completeness, a DSC test was performed on a pure octadecane sample as shown in Figure 3. Table 3 compiles the phase-change data for PCM and octadecane.

Table 3. Phase change properties of octadecane and PCM. A DSC system in step mode has been used to determine the phase change properties.

Properties		Octadecane	PCM (DSC)	PCM (DHFMA)
Enthalpy change (J/g)	Melting	224	120	123
	Solidification	212	95	95
Peak Temperature (°C)	Melting	27	26	26
	Solidification	25.5	25	25
Sub-cooling (°C)		1.5	1	1

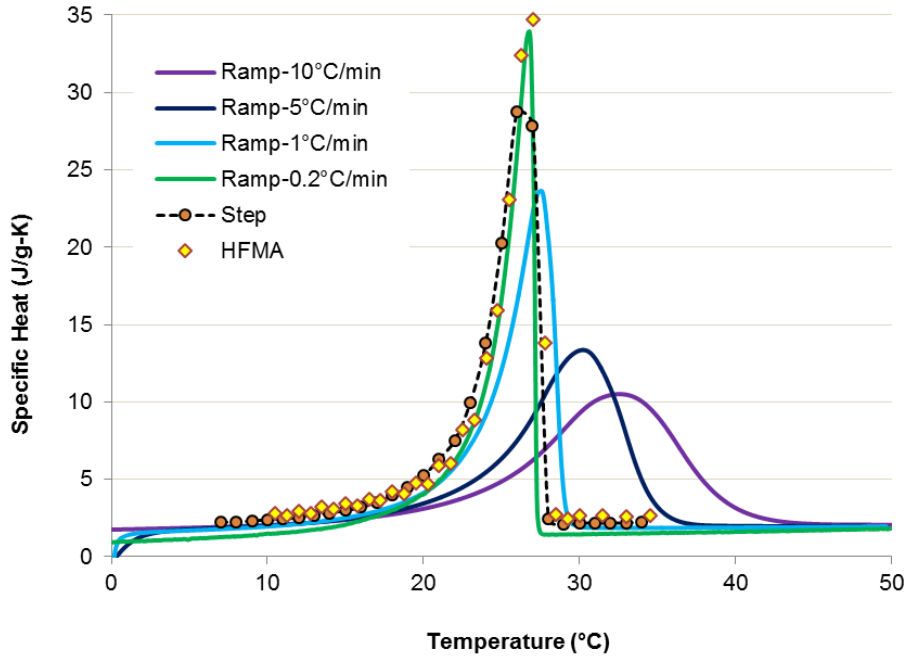

Figure 8. Specific heat as a function of temperature during melting for PCM. DSC tests were performed on a small-scale sample, while DHFMA method was performed on a large-sized sheet sample.

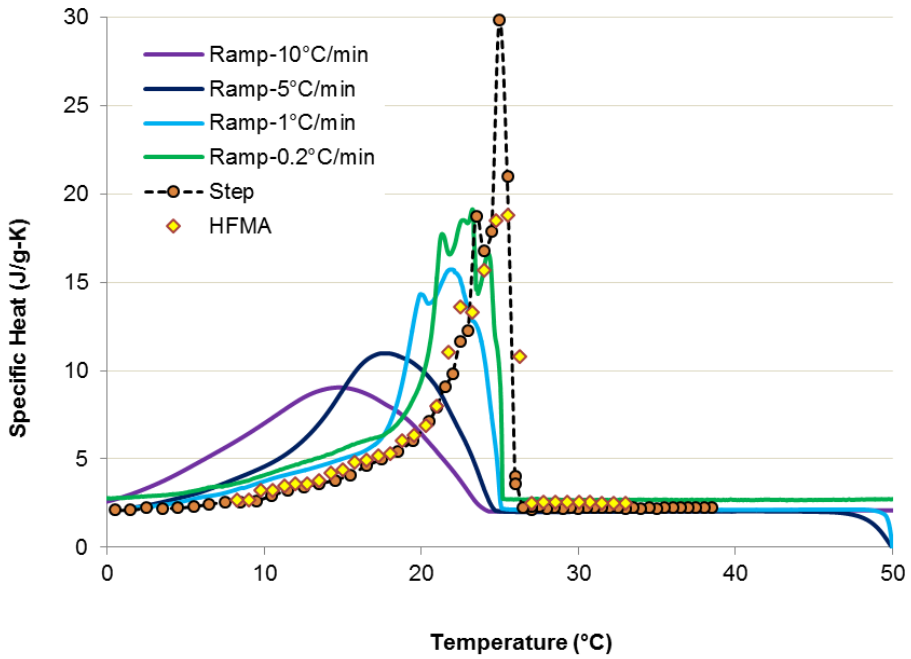

Figure 9. Specific heat as a function of temperature during solidification for PCM. DSC tests were performed on a small-scale sample, while DHFMA method was performed on a large-sized sheet sample.

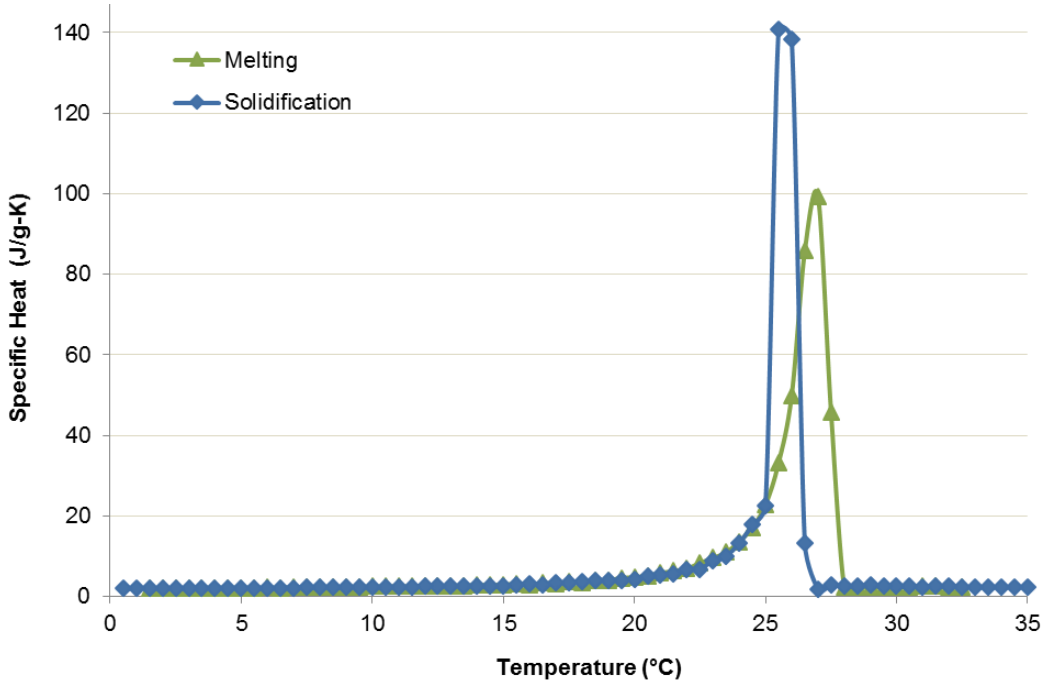

Figure 10. Specific heat of octadecane sample during melting and solidification, from step-mode DSC tests.

5. SUMMARY AND CONCLUSIONS

Field and laboratory tests of a low-cost PCM were performed and the main findings are presented in this report. The PCM installed in the test walls showed potential for energy savings, compared to conventional cellulose insulation. Interestingly, the addition of HDPE pellets

(without PCM) also showed improved thermal performance compared to cellulose-only insulation. Laboratory-scale tests to characterize the phase change properties of the PCM were also performed and have been reported. Both the field and laboratory test data are invaluable for development and validation of numerical models of PCM-containing building envelopes, which are essential for evaluating and estimating the actual energy-saving potential of PCMs.

6. ACKNOWLEDGEMENTS

The Renewable Energy Group (formerly Syntroleum) and ORNL portions of the work were funded by the United States Department of Energy as part of the American Recovery and Reinvestment Act, as Contract No. DE-EE0003924. The authors are also thankful to Jerald Atchley and Phillip Childs of ORNL for their contributions in installing and instrumenting the test wall, data gathering and troubleshooting.

7. REFERENCES

1. Kosny, J., Yarbrough, D. W., Miller, W. A., 2007. "Use of PCM Enhanced Insulation in the Building Envelope," Oak Ridge National Laboratory, Oak Ridge, TN.
2. Kosny, J., Biswas, K., Miller, W., Kriner, S., 2012. "Field Thermal Performance of Naturally Ventilated Solar Roof with PCM Heat Sink," Solar Energy, v 86, n 9, p 2504-2514.
3. B. Zalba, JM Marın, LF Cabeza, H Mehling, 2003. Review on thermal energy storage with phase change: materials, heat transfer analysis and applications. Applied Thermal Engineering, 23:251-283.
4. A Sharma, VV Tyagi, CR Chen, D Buddhi, 2007. Review on thermal energy storage with phase change materials and applications. Renewable and Sustainable Energy Reviews, 13:318–345.
5. Kosny J, Shukla N, Fallahi A. 2013. Cost analysis of simple phase change material-enhanced building envelopes in southern U.S. climates, Report for U.S. Department of Energy, Fraunhofer CSE, available online at http://cse.fraunhofer.org/Portals/55819/docs/ba_pcm_enhanced_building_envelopes.pdf
6. Shukla N, Cao P, Kosny J (2013). Lab-scale Dynamic Thermal Testing of PCM-enhanced Building Materials. ASTM Selected Technical Paper (STP) – C16 Symposium on Next-Generation Thermal Insulation Challenges and Opportunities 2013, Jacksonville, FL, Oct 23-24, 2013.
7. E Günther, S Hiebler, H Mehling, R Redlich, 2009. Enthalpy of Phase Change Materials as a Function of Temperature: Required Accuracy and Suitable Measurement Methods. International Journal of Thermophyics 30:1257–1269.